SAND2022-1061C

Postclosure Transient Criticality Analysis for a Dual-Purpose Canister

Alex Salazar III
Sandia National Laboratories
Albuquerque, NM
alesala@sandia.gov

[Digital Object Identifier (DOI) placeholder – to be added by ANS during production]

ABSTRACT

The postclosure criticality safety assessment for the direct disposal of dual-purpose canisters (DPCs) in a geologic repository includes considerations of transient criticality phenomena. The power pulse from a hypothetical transient criticality event in an unsaturated alluvial repository is evaluated for a DPC containing 37 spent pressurized water reactor (PWR) assemblies. The scenario assumes that the conditions for baseline criticality are achieved through flooding with groundwater and progressive failure of neutron absorbing media. A preliminary series of steady-state criticality calculations is conducted to characterize reactivity feedback due to absorber degradation, Doppler broadening, and thermal expansion. These feedback coefficients are used in an analysis with a reactor kinetics code to characterize the transient pulse given a positive reactivity insertion for a given length of time. The time-integrated behavior of the pulse can be used to model effects on the DPC and surrounding barriers in future studies and determine if transient criticality effects are consequential.

Key Words: dual-purpose canister, spent nuclear fuel, transient criticality, neutronics, kinetics

1 INTRODUCTION

Modeling the power pulses from hypothetical transient criticality events can provide insight on post-closure safety in an unsaturated alluvial repository. Key primary parameters of interest are the power, fuel temperature, and water temperature evolution over time. A reactor kinetics calculation with the RAZORBACK code [1] can illuminate the pulse characteristics given the material properties of the spent nuclear fuel and infiltrated groundwater along with the particular reactivity insertion characteristics. A preliminary series of a steady-state criticality calculations with the Monte Carlo N-Particle Transport (MCNP) code [2] is conducted to characterize reactivity feedback provided the conditions for baseline criticality are achieved. These feedback coefficients are used in the kinetics analysis to characterize the transient pulse given a positive insertion of reactivity for given length of time. The time-integrated behavior of the pulse can be used to model effects on the DPC and surrounding barriers in future studies and determine if transient criticality effects are consequential to repository performance.

2 METHODOLOGY

2.1 Model

A DPC is emplaced in an engineered barrier system (EBS) in a hypothetical unsaturated alluvium repository and becomes critical 9,000 years after disposal. A pre-criticality average canister temperature of 60 °C accounts for the decay heat after this period of cooling. [3] The groundwater flooding the canister is modeled as pure water with no dissolved species. Since the host rock is unsaturated and the DPC lies at or above the water table, fluid properties are determined at a hydrostatic pressure of 1 atm and 60 °C.

The DPC used for this study contains 37 Westinghouse 15 × 15 PWR spent nuclear fuel (SNF) assemblies and is currently stored at the Zion Nuclear Power Station. A model of the DPC is shown in

Figure 1, where assemblies are mounted in a basket made of 21 square tubes made of carbon steel joined at the corners. These tubes are about 0.8 cm thick and form 16 adjoining void spaces when welded, creating a total of 37 insertion channels with a center-to-center pitch of ~11.8 cm. Outside of the basket, the structural trusses joining the basket to the stainless-steel canister are modeled as empty space filled with fluid. The canister is initially backfilled with helium for storage, and then assumed to be flooded with pure water when breached 9,000 years after disposal. The inner radius of the canister circumscribes the edges of the basket, where an assumed thickness of 1.25 cm results in an outer radius is 91.5 cm. The canister is placed into a 5 cm thick 316 stainless steel overpack, which is surrounded by the EBS.

The tubes contain four absorber assemblies of boron carbide (B_4C)/aluminum composite plates mounted internally with stainless steel retainers. The adjoining void spaces do not contain absorber assemblies. The composite is assumed to contain 65 at% B_4C (43.2 wt%), with boron comprised of the natural abundance of 81.6 wt% B-11 and 18.4 wt% B-10. The aluminum component is assumed to be pure ^{27}Al metal with no oxide, and the constituent atoms of the absorber are modeled as a homogeneous mixture.

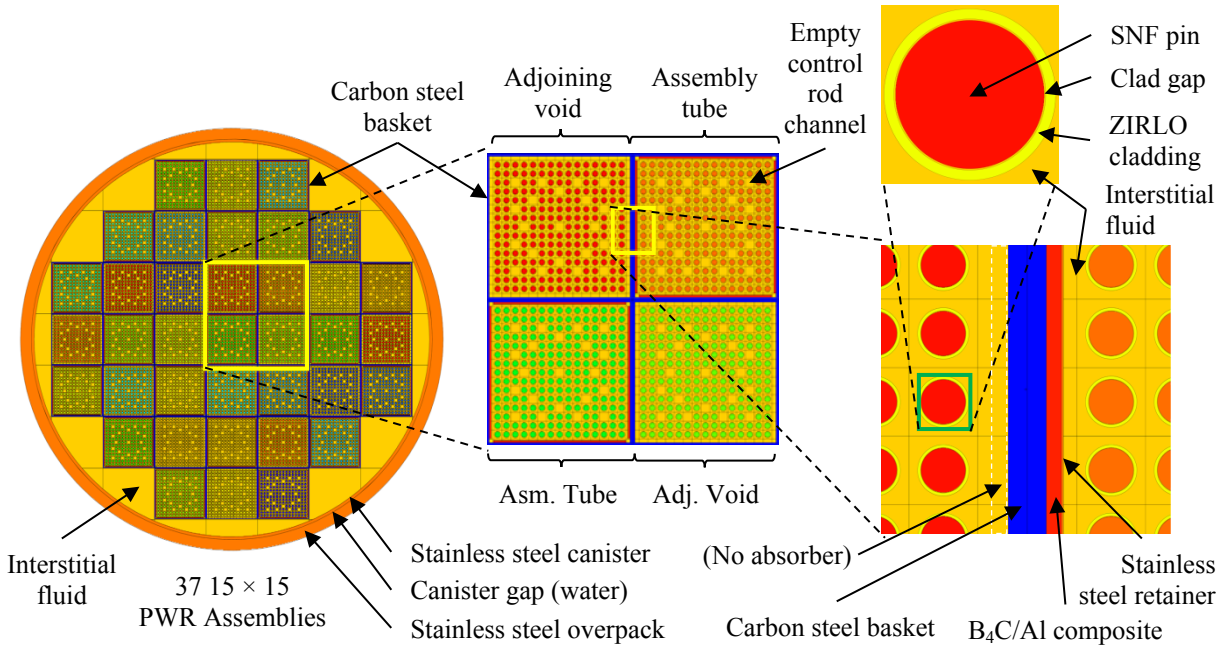

Figure 1. Radial model of DPC used in the MCNP simulations

Fresh fuel dimensions (i.e., prior to reactor operation) are assumed as a conservatism for the neutronics analysis. The fuel rods consist of UO_2 fuel pellets surrounded by a fluid-filled gap and ZIRLO (a zirconium-based alloy) cladding. The fuel has a density (ϱ) of 10.2 g/cm^3 (93% of theoretical). The rods and guide tubes are separated by a center-to-center pitch of 1.4 cm and have a uniform length of 400 cm, where the fuel and cladding edges are assumed to be flush with no plenum regions or springs. Dishing of fuel pellets and gaps between fuel pellets are ignored, making the fuel a continuous cylindrical volume. The SNF is assumed to be disposed with no control rods, allowing for an inspection of the full excess reactivity of the canister. The grid spacers, guide tubes, tie plates, and other nonfuel components (while present physically) are ignored in the neutronics model and replaced with water. The longitudinal extents of the DPC are non-prototypic and devised to reduce effects of asymmetry in the results. The assemblies are modeled as lying within the center of the tube with fluid filling the void spaces above and below. There are also fluid-filled gaps between the basket and canister lid and between the canister and overpack.

2.2 Fuel Composition

The fuel composition was provided by Oak Ridge National Laboratory from depletion calculations on

an assembly basis for a cask at Zion. Emplacement was assumed at calendar year 2100 and results were postprocessed for direct use in MCNP. The median operational values for the assemblies are 2.81 wt% initial enrichment, 455.0 kg initial uranium, 27.9 GWd/t burnup, and 122.4 years cooling time after reactor discharge (around 1977). The span of discharge dates is between 1975 and 1996, while burnup ranges from 17.4 to 38.6 GWd/t and initial enrichment ranges from 2.24 wt% to 3.56 wt%. The as-loaded configuration of the DPC has assemblies with higher initial enrichments and burnups around 22.5 GWd/t biased towards the center, while the lowest initial enrichments and burnups are placed on the periphery. The content of most fissile isotopes at 9,000 years appears to be concentrated near the center of the DPC. The maximum fissile content at this time is 2.33 wt% although the median value is only 1.54 wt%. Normalized mass fractions were generated for all unique nuclides per assembly per time point, and nuclides with mass fractions above 10^{-8} were passed to the neutronics analysis (36 nuclides). On average, at 9,000 years, the material consists of 99.5 wt% actinides with 98.7 wt% uranium and 0.6 wt% plutonium. Notable poisons ^{149}Sm and ^{155}Gd are present in small quantities, but there are also other stable fission products with appreciable absorption cross sections.

2.3 Neutronics

The MCNP code (version 6.1.1) is used to evaluate effective multiplication (k_{eff}) in the DPC using the canister model and Zion inventories. [2] The code and its cross-section libraries have been benchmarked for low-enriched uranium (< 10 wt%) criticality studies via data from the International Criticality Safety Benchmark Evaluation project handbook. [4] For criticality calculations, source points are defined that represent neutrons from spontaneous fission or neutrons emitted as a result of decay. Static calculations maintain cross sections from the Evaluated Nuclear Data File/Version B – Rev. 7.1 library at 20.45 °C. Calculations incorporating effects of Doppler broadening modify cross sections in the fuel as the temperature increases using the On-the-Fly Doppler Broadening (OTFDB) code. [5] Scripts were used to calculate evolving material compositions and fluid densities and to modify input files.

2.4 Criticality scenario

The criticality scenario involves a progressive state of internal DPC degradation. After some period in storage, the DPC is emplaced in an alluvial repository surrounded by an overpack and EBS. Upon emplacement, the canister is subject to corrosion and other phenomena that can result in a breach and subsequent water infiltration. Extensive degradation of packaged neutron absorbers is then required for infiltrated water to impart increases in system reactivity (ρ). The absorbers are hypothesized to degrade first, followed by other components such as the canister basket and assembly hardware.

The model follows the as-loaded configuration of assemblies and includes the effects of the basket and neutron absorbers but ignores the effects of the structural components of the assemblies (i.e., grid spacers, tie plates, guide tubes, etc.) The water level in the breached DPC is susceptible to change as it is emplaced above the water table. Water can infiltrate a breach and submerge the SNF to a certain level, but it may also evaporate and exfiltrate the canister in a cyclic manner given heating from decay and criticality. Nonetheless, this study will consider a fully-flooded canister as part of an initial criticality scoping analysis.

While the composite neutron absorber material is strongly resistant to aqueous dissolution, suspensions of small, solid particles may be susceptible to transport and provide a mechanism for displacing absorbers from their original location. In a situation where the DPC is heavily tilted or inverted due to erosion or seismic events, B_4C particles from mechanically-degraded absorbers can be displaced from their original positions around the SNF. A worst-case scenario would have these particles traverse the length of the tube and accumulate outside of the fuel, removing shielding between fuel rods in neighboring assemblies and increasing reactivity in the DPC. This study will apply this full displacement scenario, where engineered absorbers are gradually replaced with water and effectively removed from neutron transport, constituting a reactivity insertion.

2.5 Reactivity Feedback

Reactivity feedback from the introduction of water, loss of absorber, and changes in DPC configuration is provided through a series of steady-state neutronics analyses. Additional feedback mechanisms are explored that include increasing temperature in the fuel, thermal expansion in the fuel, and voiding of the moderator. The increase in fuel temperature is hypothesized to reduce system reactivity through Doppler broadening, which describes a smearing effect of resonances with increasing average temperatures. The peaked resonances for absorption are broadened in energy as a consequence of increased vibrational motion in the target nuclei. This results in a depression in absorption cross-section peaks and a spread in the range of applicable energies, where the latter effect ultimately leads to a net increase in absorptions.

For calculations incorporating Doppler broadening effects, the cross sections in the fuel are modified with evolving temperature using the OTFDB code. The code uses ENDF data at various temperatures to create an interpolated energy grid based on a temperature range with set intervals. When a collision is scored in MCNP, OTFDB employs the specific cell temperature to alter both the collision kinematics and absorption cross sections based on the Cullen and Weisbin exact Doppler broadening equation. [6]

There are 54 unique nuclides across all materials at 9,000 years. A script was written to run the preprocessor code for these nuclides and create interpolations based on a range of temperatures from 300 K (26.85 °C) to 2,500 K (2,226.85 °C). The 300 K lower bound is used for rounding purposes, as related ENDF-B/VII.1 evaluations in MCNP include those at 293.6 K and 2,500 K. The upper bound temperature is below the melting point of pure UO_2 fuel (around 2,800 °C) but lies above the expected melting point of 2,000 °C for zirconium-based alloys. Therefore, the final temperatures in the analysis should cover the point where significant fuel rod degradation is achieved and a transient criticality event would not be sustainable. Eighth order interpolations are made in 10 K intervals across this temperature range using an energy grid based on 100 K bins.

RAZORBACK employs the temperature feedback coefficient in the form of the power law shown in Eqn. (1). The coefficients $\mathcal{C}_0$ and $\mathcal{C}_1$ are fitted to the results of the static MCNP calculations with OTFDB to provide an approximation of the temperature feedback coefficient.

$$\partial\rho/\partial T = \mathcal{C}_0 + \mathcal{C}_1/\sqrt{T} \tag{1}$$

The code also employs feedback coefficients for the coolant in terms of increasing temperature ("spectral") and voiding. The coolant temperature coefficient is implemented as reactivity per Kelvin while the voiding coefficient is implemented as reactivity per percent void. In the MCNP simulation, the temperature feedback coefficient is obtained by increasing coolant temperature and modifying coolant density up to 100 °C at 1 atm (pure vapor data are considered unimportant for the transient). The voiding coefficient is found by increasing the steam quality at the 1 atm saturation temperature and using the homogenized density. While the characteristics of two-phase flow would be strongly influenced by the canister geometry and the level of steam separation, the analysis treats the mixture as homogeneous throughout the void space.

The gap can be modeled as being filled with helium (unbreached) or water (from water infiltration). The latter is more representative of the failed state, as rods would eventually be breached from corrosion, but the former is a conservative choice for more accurately portraying the role of thermal expansion in the thermal system. The water properties in the coolant analysis are obtained from the IAPWS Industrial Formulation 1997 (IF97) for the Thermodynamic Properties of Water and Steam. [7] The open-source CoolProp thermophysical property database (version 6.4.1) is used to evaluate this specific formulation and also provide thermophysical data for helium. [8]

2.6 Reactor Kinetics

RAZORBACK is a reactor transient analysis code designed to determine the response of a pool-type natural circulation research reactor via a coupled numerical solution of the point kinetics equations, the conservation of energy, and the conservation of momentum for coolant and fuel elements. [1] It has been validated for transient analyses with data from the Sandia National Laboratories (SNL) Annular Core

Research Reactor. [9] In this study, it is used to evaluate the point kinetics equations given the reactivity feedback behavior in the DPC provided by the neutronics analysis, as it is compatible with the hydrostatic pressure in the alluvium repository. Calculations are meant to span the applicable time period of the postulated transient pulse for a given total reactivity insertion. In this model framework, a baseline critical state is assumed before the transient, although in-situ events may theoretically proceed from a sub-critical state.

In the simulation, the flooded DPC functions as a reactor when absorber plates are compromised, where the maximum power is modeled as 1 MW. The problem employs all 7,548 SNF rods in the DPC and utilizes an element peak-to-average factor of 1.5096 to impart a maximum element power of 20 kW for power fraction. Before the transient begins, the problem is allowed to stabilize for 60 seconds with no feedback or reactivity insertion. It then initiates at 100.0% of the full reactor power, with the reactivity insertion beginning at time zero.

The code features reactivity controls in the form of a control rod (CR) bank, safety rod bank, and transient rod bank, all of which follow the same time- and space-dependent behavior (although the transient rods have additional features). The calculations presented here only use the control rods as means of controlling the time-dependent reactivity insertion. Use of the control rod bank required construction of a differential reactivity curve as a sine-squared function based on the axial height. While this information can be obtained from neutronics, this study assumes a curve that is nearly linear across the fuel rod. The curve parameters were also adjusted to integrate to unity across the whole extent of the fuel so the curve could be scaled to the total worth of the control rod bank, with the resulting function shown in Eqn. (2). The control rod is withdrawn at a fixed speed to a certain distance to insert the desired worth within a given time period.

$$d\rho/dz|_{CR}[cm^{-1}] = 0.0105652 \cdot \sin^2(0.00004 \cdot z + 0.5) \quad (2)$$

While the DPC is horizontally emplaced, the problem requires the configuration to be vertical to follow the engineered reactor basis of the code and to allow the assemblies to be directly exposed to a column of water acting as a coolant channel in a virtual "tank." The pool tank height is set as 1,060 cm, providing a maximum 626 cm water column above the coolant channel and 640 cm above the top of the fuel. The water column determines the pressure at the bottom and top of the coolant channel assuming 14.696 psia hydrostatic pressure at the top. This study assumes a water level at 300 cm below the tank lip, which implies 326 cm of water in the coolant channel and a pressure range from 19.3 psia to 25.5 psia. The tank area of 25,543.1 cm^3 represents the area from inner canister radius. There is no other displaced volume in the water apart from the reactor. The pool heating is determined by the DPC power output and natural convection, and the initial pool temperature is 60 °C.

The fuel is modeled with three zones: cylindrical UO_2 fuel, a clad gap filled with water or helium, and ZIRLO cladding. The clad gap is a necessary initial condition to explore thermal expansion and radiative heat transfer effects in the kinetics study; however, this assumption is not representative of the deformed state of SNF. Dimensions are borrowed directly from the neutronics analysis including the non-prototypic fuel length of 400 cm. Pressure inside and outside of the fuel element is set initially at 14.696 psia (101,325 Pa), although the outer pressure is fixed. The fuel is divided into a number of radial and axial nodes. The coolant channel has a heated region adjacent to the fuel elements and unheated regions 14 cm above and 20 cm below the fuel, providing a total system length of 434 cm. The coolant node inlet/exit flow area is 1.36656 cm^2 with a wetted perimeter of 1.45988 cm.

Table I shows material properties of the fuel element components as implemented in the RAZORBACK simulation. The densities of UO_2 and ZIRLO are carried over from the neutronics analysis, while the densities of the fluids are obtained at 20 °C. The MELCOR database is used to determine temperature-dependent thermal conductivity and specific heat for UO_2 and ZIRLO (via Zircaloy). [10] Two different temperature ranges are used to define κ_T and c_p for UO_2, where the melting point of 3,113 K marks a transition point for evaluating constant values for the melt. This behavior is applied as a piecewise equation with a polynomial for the solid region and a constant for the melted one.

Table I. Material properties at 101,325 Pa for a fuel element

Property \ Material	UO_2	Water	Helium	ZIRLO
Density at 20 °C (g/cm³)	10.2	0.998206092	0.000166311	7.75
Thermal Conductivity (W/[cm·K])	MELCOR	IF97	CoolProp	MELCOR
Specific Heat Capacity (J/[g·K])				
Thermal Radiation Surface Emissivity	0.8	0.95	1.0	0.325
Thermal Radiation Transmissivity	0.0	1.0	1.0	0.0
Linear Thermal Expansion Coefficient (K^{-1})	Eqn. (3)	0.0[a]	0.0[a]	6.721E-6
Young's Modulus (GPa)	180	1.0E-20[b]	1.0E-20[b]	89.9
Poisson's Ratio	0.303	0.3[b]	0.3[b]	0.35

[a] RAZORBACK does not expand fluids | [b] Recommended values for gas in RAZORBACK

For UO_2, the linear strain from thermal expansion is found from a temperature-dependent fit. [11] The linear strain is evaluated from 273.15 K to 2,500 K and then fitted to a second order polynomial function of temperature (in Kelvin). The derivative of this fit is then taken as the linear thermal expansion coefficient, as shown in Eqn. (3). For the remaining UO_2 properties, a transmissivity of 0.0 is used to follow the RAZORBACK convention of applying this value for solids; a value of 1.0 is used for gases, where water is assumed to enter the vapor phase during the transient. For ZIRLO, the strain from thermal expansion was obtained from a radial fit of Zircaloy data. [11] The strain was evaluated from 273.15 to 2,500 K and then fitted to a line, with the slope providing the thermal expansion coefficient of 6.721×10^{-6}.

$$\alpha(T)[K^{-1}] = 5.333 * 10^{-6} + 5.078 * 10^{-9}\, T \tag{3}$$

3 RESULTS

3.1 Neutronics

The storage phase serves as a baseline reference case for the subcritical state before the effects of water flooding can be considered. Here, the DPC is modeled with a backfill of 95 at% (83.9 wt%) helium and 5 at% (16.1 wt%) air at 60 °C and 8 bar. Subcritical conditions are confirmed with a k_{eff} of 0.30167 ± 0.00013 at emplacement and 0.29753 ± 0.00013 after 9,000 years of decay (and no loss of pressure).

The k_{eff} in the DPC is evaluated as the absorber/retainer assemblies are degraded according to the full displacement scenario. The system begins in subcritical conditions when the DPC is flooded and the absorbers are intact, where k_{eff} is 0.86303 ± 0.0003 (ρ = -0.15871). The value of k_{eff} steadily increases as more absorber is degraded, with the complete degradation state lying at 1.02848 ± 0.00029. The weighted mean of the delayed neutron fraction is 0.00547 ± 0.00006, suggesting that a maximum dollar reactivity of $\rho_\$$ = \$5.09 is achieved when all of the absorber is degraded and transported outside of the fuel. This can be interpreted as the "worth" of the installed absorbers given a flooded DPC. Figure 2 shows the reactivity of the system as the last quantity of absorber and retainer are replaced with water. Criticality is achieved when 99.13 vol% of the absorber assembly has degraded in the flooded DPC basket. The system is prompt-critical shortly after at 99.30 vol% degradation.

The temperature feedback coefficients in the fuel and coolant were estimated in a series of neutronics calculations. For the fuel, this involved sequentially broadening the UO_2 cross sections with increasing fuel temperatures while maintaining external materials at ambient temperature. The temperature range of 300–2,500 K was used to apply the OTFDB lookup tables up to cladding failure. The analysis assumed a rapid increase in fuel temperature such that 1) no significant heat is transferred to the surroundings such that non-UO_2 components are fixed with cross sections at 300.5 K, and 2) the material properties are unaffected with the fuel geometry remaining intact.

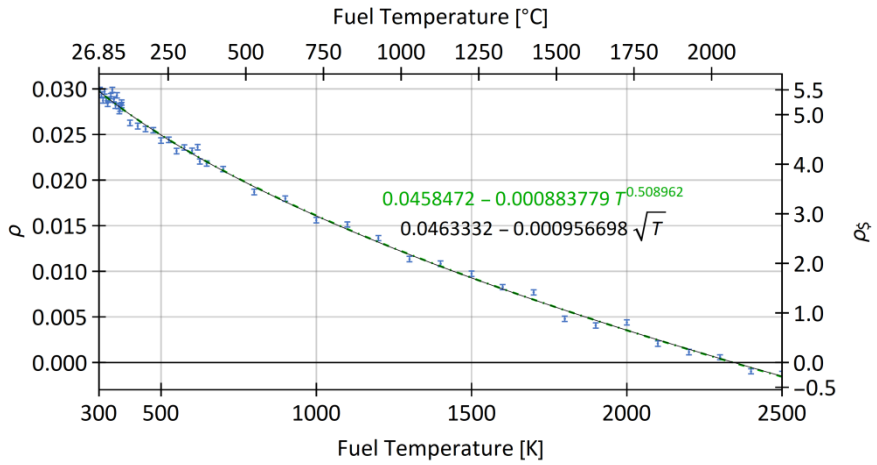

Figure 2. Reactivity as a function of fuel temperature when perturbing the UO_2 temperature. The figure shows a generic power law fit (green) and a √T fit (black) for all points.

The reactivity results are shown in Figure 2 and include a generic power law fit and a specific $\sqrt{T}$ fit aligning with Eqn. (1), although the two approaches are essentially identical. Progressing from 300 K to 2,500 K results in a reactivity drop from \$5.40 to −\$0.23, and the critical configuration is maintained until 2,337.63 K (2,064.48 °C). Therefore, the loss of criticality from Doppler broadening in the fuel with extreme heating is concurrent with the melting of cladding, which itself destroys the critical configuration.

The analysis for the coolant temperature feedback coefficient was conducted by varying the temperature and density of all water infiltrating the canister, including the fuel rod gaps, the tube/void cavities, the space outside of the basket, and the canister gaps. (Any water in the UO_2 fuel matrix was excluded.) Doppler broadening was active for the hydrogen (H-1) and oxygen (O-16) in the water. The densities for liquid water at 101,325 Pa are used up to the vapor point, terminating at 373.1243 K (99.9740 °C). For 100 °C and up, to maintain the liquid phase, it is assumed that pressure buildup allows for water to remain saturated, and the density of the saturated liquid is used up to the critical point, terminating just below 647.096 K (373.946 °C). The void coefficient is evaluated for saturated water/steam at 99.9740 °C at various steam qualities. The temperature of the water in the DPC is fixed while the density is modeled as homogenous and a function of quality.

Table II. Reactivity feedback coefficients

Mechanism	Feedback Coefficient	Units
Fuel temperature	$\partial\rho_\$/\partial T_F = -0.088017527/\sqrt{T}$	\$/K
Coolant voiding	$\partial\rho_\$/\partial(\%Void) = -3.9444568$	\$/(%void)
Coolant temperature	$\partial\rho_\$/\partial T_W = -0.0087093620$	\$/K
Fuel thermal expansion: $R_{F,o}$	$\partial\rho_\$/\partial R_{F,o} = -41.821538$	\$/cm
Fuel thermal expansion: ϱ_F	$\partial\rho_\$/\partial \varrho_F = 0.98133973$	\$/(g/cm^3)
Cladding thermal expansion: $R_{C,o}$	$\partial\rho_\$/\partial R_{C,o} = -56.471229$	\$/cm
Cladding thermal expansion: $R_{C,i}$	$\partial\rho_\$/\partial R_{C,i} = 36.070511$	\$/cm
Cladding thermal expansion: ϱ_C	$\partial\rho_\$/\partial \varrho_C = 0.35064621$	\$/(g/cm^3)

The thermal expansion coefficients are obtained by varying the fuel and cladding dimensions. These geometric changes are implemented at 300 K to de-couple temperature dependence on the expanding geometry. For the fuel, the outer radius of the UO_2 pellet was varied from the engineered specification until it pressed directly against the inner wall of the ZIRLO cladding. The total mass of fuel is maintained constant, so dimensional changes are met with a change in fuel density. When the fuel radius is at its

maximal extent, interstitial water no longer acts as a moderator between the fuel and cladding. The thermal expansion analysis was then applied to the cladding independently for both the inner radius and outer radius in separate analyses.

The total neutron generation time and β_{eff} as obtained from the absorber degradation study are 2.65808×10^{-5} seconds and 0.005443874, respectively. The reactivity feedback coefficients from the MCNP studies are summarized in Table II. The coolant temperature coefficient listed here is restricted to the liquid phase at 101,325 Pa. Also, the inner cladding radius study is used to provide the density feedback coefficient for the thermal expansion of ZIRLO.

3.2 Kinetics

The control rod bank is defined with a worth of \$5.40, which is obtained from the absorber-degraded state of the DPC as observed at 300 K in the Doppler feedback study. The differential reactivity curve from Eqn. (2) is integrated and scaled to the total worth, with Table III showing the resulting control rod bank heights for given reactivity insertions. The control rod withdrawal speed for reactivity insertion is determined using these heights along with the total insertion period. The transient was analyzed for scenarios with the clad gap filled with helium and water. Reactivity insertions between \$1 – \$5 are analyzed for periods of 10 ms, 100 ms, 500 ms, and 1 s.

Results for water and helium were mostly comparable and the maximum system-wide reactivities observed in the simulation were similar, although the H_2O scenario extended the time for the simulation to reach subcriticality. Other nuances in results exist from fits of the thermophysical properties. The results for peak power (P), energy release (E), maximum fuel temperature (MF), and peak system reactivity are shown in Table IV for the H_2O case. Some simulations do not reach subcriticality due to limitations of the coolant equation of state with rapid temperature increases from the pulse. Powers range on the order of 1×10^{9} W to 4×10^{12} W and integrated energies up to the time of subcriticality (or the end of the simulation) range from 1×10^{9} J to nearly 10^{10} J. For a given insertion period, the time at which the peak power occurs decreases as the CR worth increases. The maximum fuel temperatures do not appear to reach the melting point of the cladding, with a maximum of 1885 °C observed with the \$3 insertion over 1 s.

Figure 3 shows the time evolution of power (on a $\log_{10}$ scale), fuel temperature, and reactivity feedback for the \$1 reactivity insertion over 1 second with the H_2O-filled gap. After the control rod is withdrawn, the power pulse reaches a peak of 1.39 GW ($\log_{10}$ of 9.14) before slowly decaying towards the 1 MW initial condition. The maximum fuel temperatures lag the time of peak power due to heat transfer limitations, where a temperature of 478 °C is observed at subcriticality and a maximum of 518 °C before the end of the simulation. After the control rod withdrawal, negative feedback mechanisms exist most predominantly from the coolant. While not resolved on the plot, the coolant briefly provides positive feedback due to a transient increase in the channel pressure before becoming negative as temperature increases with steady pressure. Feedback from the temperature and thermal expansion of the fuel are the next most negative, followed by thermal expansion of the cladding. This suggests that heating of the flood water and fuel in the DPC can sufficiently terminate chain reactions given significant absorber failure.

Table III. Control rod bank positions per given reactivity insertion

Total Reactivity Insertion $\rho_{\$}$ [\$]	CR Bank Position [cm]
1	74.9567
2	149.506
3	223.653
4	297.404
5	370.764
5.40 (full worth)	400.000

Table IV. Transient pulse results up to subcriticality for fuel element with H_2O-filled gap.

t (s)	$1	$2	$3	$4	$5
0.01	P: 1.58E+09 W E: 1.35E+09 J MF: 494.12 °C ρ: 1.005	P: 5.90E+11 W E: 5.34E+09 J MF: 1651.77 °C ρ: 2.009*	P: 1.72E+12 W E: 5.67E+09 J MF: 1726.25 °C ρ: 3.002*	P: 2.06E+12 W E: 3.91E+09 J MF: 1240.50 °C ρ: 4.012*	P: 3.98E+12 W E: 5.79E+09 J MF: 1736.42 °C ρ: 5.018*
0.1	P: 1.46E+09 W E: 1.31E+09 J MF: 486.83 °C ρ: 1.000	P: 4.68E+11 W E: 3.65E+09 J MF: 1079.39 °C ρ: 1.999*	P: 1.46E+12 W E: 5.24E+09 J MF: 1616.33 °C ρ: 2.607*	P: 1.88E+12 W E: 5.63E+09 J MF: 1711.93 °C ρ: 2.902*	P: 1.80E+12 W E: 4.50E+09 J MF: 1409.60 °C ρ: 3.162*
0.5	P: 1.41E+09 W E: 1.30E+09 J MF: 479.62 °C ρ: 1.000	P: 1.98E+11 W E: 8.22E+09 J MF: 1677.49 °C ρ: 1.455	P: 3.07E+11 W E: 3.74E+09 J MF: 1188.86 °C ρ: 1.591*	P: 3.32E+11 W E: 3.00E+09 J MF: 925.60 °C ρ: 1.711*	P: 5.91E+11 W E: 5.76E+09 J MF: 1722.40 °C ρ: 1.821*
1	P: 1.39E+09 W E: 1.28E+09 J MF: 477.88 °C ρ: 0.998	P: 7.92E+10 W E: 5.23E+09 J MF: 1604.70 °C ρ: 1.277	P: 1.33E+11 W E: 6.35E+09 J MF: 1884.56 °C ρ: 1.372	P: 1.86E+11 W E: 9.93E+09 J MF: 1515.08 °C ρ: 1.455	P: 2.57E+11 W E: 4.10E+09 J MF: 1324.67 °C ρ: 1.526*

* Simulation did not reach subcriticality, so energies are based on the end time of simulation

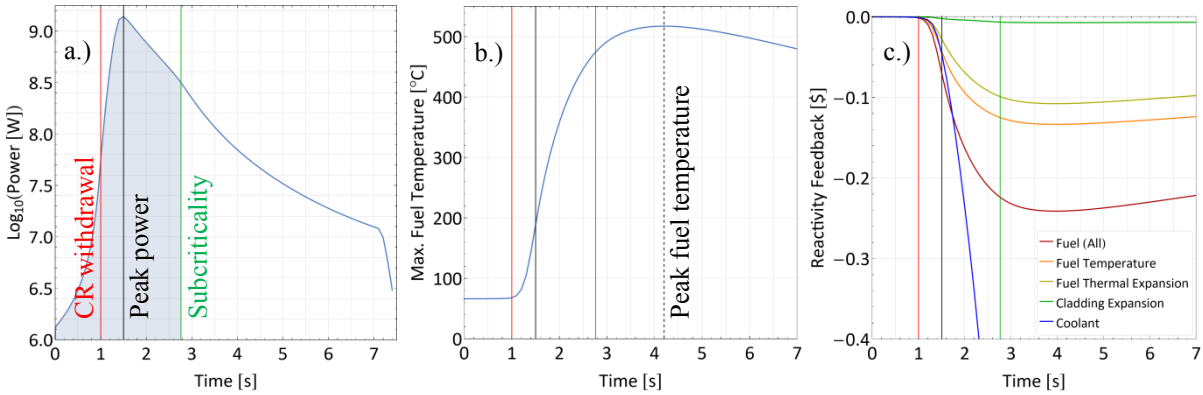

Figure 3. Results for a) power, b) max fuel temperature, and c) feedback for H_2O-filled gap, $1, 1 s case.

4 CONCLUSIONS

It has been demonstrated that reactivity insertions can be modeled in a transient analysis for a DPC if it is assumed that packaged absorbers function analogously to reactor control rods. If these absorbers disintegrate within a short time period, the resulting reactivity insertions result in rapid releases of energy on the order of 10^9 – 10^{10} J within a span of a second. Results can be compared to known reactivity-initiated accidents to check for consistency. If the total number of fissions deduced from the energy output are deemed of concern, the next phase of the analysis can apply the transient kinetics results to a solid mechanics study using a simplified DPC and barrier system.

The MCNP model can be improved by adding axial discretization, which will allow for 1) development of more representative differential reactivity curves and 2) investigation of the distribution of fission energy via a depletion study. Additionally, accommodating individual rod fidelity to temperature and density can support an assessment of the fission power distribution across the DPC, a study of power-peaking factors, and investigations of varying water levels in unsaturated geology. The RAZORBACK simulation can benefit from employing characteristics more representative of SNF (as opposed to fresh UO_2). It may be possible to obtain these properties from site measurements of the fuel from Zion. Refinements are also needed for characterizing feedback from thermal expansion specifically in SNF.

5 ACKNOWLEDGMENTS

The author would like to acknowledge Laura L. Price (SNL) for her review of this paper. This research was funded by the US Department of Energy, Office of Nuclear Energy under the Spent Fuel and Waste Science and Technology campaign. This paper describes objective technical results and analysis. Any subjective views or opinions that might be expressed in the paper do not necessarily represent the views of the U.S. Department of Energy or the United States Government. Sandia National Laboratories is a multimission laboratory managed and operated by National Technology & Engineering Solutions of Sandia, LLC, a wholly owned subsidiary of Honeywell International Inc., for the U.S. Department of Energy's National Nuclear Security Administration under contract DE-NA0003525. SAND2022-XXXXX.

This is a technical paper that does not take into account contractual limitations or obligations under the Standard Contract for Disposal of Spent Nuclear Fuel and/or High-Level Radioactive Waste (Standard Contract) (10 CFR Part 961). For example, under the provisions of the Standard Contract, spent nuclear fuel in multi-assembly canisters is not an acceptable waste form, absent a mutually agreed to contract amendment. To the extent discussions or recommendations in this paper conflict with the provisions of the Standard Contract, the Standard Contract governs the obligations of the parties, and this paper in no manner supersedes, overrides, or amends the Standard Contract. This paper reflects technical work which could support future decision making by DOE. No inferences should be drawn from this paper regarding future actions by DOE, which are limited both by the terms of the Standard Contract and Congressional appropriations for the Department to fulfill its obligations under the Nuclear Waste Policy Act including licensing and construction of a spent nuclear fuel repository.

6 REFERENCES

1. D. G. Talley, *RAZORBACK – A Research Reactor Transient Analysis Code v. 1.0 vol. 1: User's Manual*, SAND2017-10561, Sandia National Laboratories, Albuquerque, NM (2017).
2. T. Goorley, *MCNP6.1.1-Beta Release Notes*, LA-UR-14-24680, Los Alamos National Laboratory, Los Alamos, NM (2014).
3. L. L. Price *et al*., *Preliminary Analysis of Postclosure DPC Criticality Consequences*, SAND2020-4106, Sandia National Laboratories, Albuquerque, NM (2019).
4. J. B. Briggs, L. Scott, and A. Nouri, "The International Criticality Safety Benchmark Evaluation Project," *Nucl. Sci. Eng.*, **145(**1), pp. 1–10 (2003).
5. W. Martin*, Implementation of On-the-Fly Doppler Broadening in MCNP5 for Multiphysics Simulation of Nuclear Reactors*, NEUP 10-897, Battelle Energy Alliance, Ann Arbor, MI (2012).
6. D. E. Cullen and C. R. Weisbin, "Exact Doppler Broadening of Tabulated Cross Sections," *Nucl. Sci. Eng.*, **60**(3), pp. 199–229 (1976).
7. W. Wagner *et al*., "The IAPWS Industrial Formulation 1997 for the Thermodynamic Properties of Water and Steam," *J. Eng. Gas Turbines Power*, **122**(1), pp. 150–184 (2000).
8. I. H. Bell *et al.*, "Pure & Pseudo-pure Fluid Thermophysical Property Evaluation & the Open-Source Thermophysical Property Library CoolProp," *Ind. Eng. Chem. Res.*, **53(**6), pp. 2498-2508 (2014).
9. D. G. Talley, *RAZORBACK – A Research Reactor Transient Analysis Code v. 1.0 vol. 3: Verification and Validation Report*, SAND2017-3372, Sandia National Laboratories, Albuquerque, NM (2017).
10. L. L. Humphries, V. G. Figueroa, M. F. Young, D. Louie, and J. T. Reynolds, *MELCOR Computer Code Manuals*, SAND2015-6692R, Sandia National Laboratories, Albuquerque, NM (2015).
11. OECD Nuclear Energy Agency, *Reactivity-Initiated Accident Fuel-Code Benchmark Phase II Volume 2: Task No. 1 Specifications*, NEA/CSNI/R(2016)6/VOL2, Paris, France (2016).